Structure and Reaction in the Active Site of Mammalian Adenylyl Cyclase

Yong-Sok Lee[†] **and Morris Krauss***[,‡]

Center for Molecular Modeling, CIT, National Institutes of Health, Bethesda, Maryland 20892, and Center for Advanced Research in Biotechnology, NIST, Rockville, Maryland 20850

Received: August 28, 2003; In Final Form: January 31, 2004

The reaction path for the catalytic conversion of adenosine triphosphate (ATP) to cyclic adenosine monophosphate (cAMP) by the enzyme mammalian adenylyl cyclase has been calculated theoretically using the Hartree−Fock method. The crystal structure of a thiophosphate reactant analogue, ATPαS, provides the basic structure of the active site binding that is then leveraged into the native reaction path by energy gradient optimization of protein binding residues and the ATP. A two-metal cluster bound to two aspartate residues and the ATP is important both structurally and catalytically. Autocatalytic activation of the reacting ribose 3′OH group is calculated in the reactant conformation but the catalytic MgA divalent cation binds to the developing 3′O anion and stabilizes the formation of a five-coordinate intermediate with the cyclic phosphate already formed. Changes in the coordination of the metals in the complex and the H-bonding of arginines that bridge the phosphate groups stabilize the reaction path complex from reactive intermediate to the product. Final transfer of the 3′H proton to the oxygen bridging the α and *β* phosphate groups yields the cAMP and pyrophosphate product still bound by many H-bonds in the active site.

1. Introduction

Cyclic adenosine monophosphate (cAMP) is an important messenger in hormone signaling. Understanding the mechanism of production of cAMP from adenosine triphosphate (ATP) by the adenylyl cyclase (AC) family of enzymes has advanced recently through the determination of the binding of a number of reactant and product analogues in the ATP active site of AC. The ATP binding active site is constructed with residues contributed by two distinct domains and two divalent metal cations binding to ATP. A two-metal-ion catalytic mechanism has been deduced from these structures[1−3] and mutagenesis data.[4,5] However, the structural data either raises or cannot answer significant questions regarding the atomic level mechanism. The native reaction path cannot be determined at the atomic level from inhibitors that are at best analogues of the reactive structures along the path. Significant questions exist: (1) How is the ribose 3′-OH activated? (2) How is the developing charge on the 3′-O anion stabilized? (3) What is the function of the two-metal structure? (4) What is the detailed coordination behavior of the metals? (5) Which, if any, binding residues are catalytic? (6) Are the native substrate and product structures distorted by binding in the active site? This information cannot easily be obtained from the available experimental structures. Although all the experimental structures find the analogue inhibitors are bound to the same two-metal complex and protein residues, the atomic description of the active sites are necessarily different. This is due to the presence of thiophosphate in one case, the lack of ribose hydroxyl groups in the other, and the variety of metals used.[1,3]

The essential steps along the reaction path in the production of cAMP from ATP are described in Figures 1a, 2a, and 3a. These figures were obtained from the optimized structures for the reactant, intermediate, and product calculated as described below. The activation of the ribose 3′OH by H-bonding to the Pα oxygens is seen in Figure 1a. The 3′OH is dissociated with the H binding to the Pα phosphate oxygen whereas the 3′O binds to the phosphorus as seen in Figure 2a. Binding of 3′O to Pα creates the cyclic phosphate and the product is then obtained by binding the 3′H to the bridging oxygen between the Pα and P*β* and breaking the P*β*-O bond, as seen in Figure 3a for the product.

From the available experimental information, the mechanism for activation and deprotonation of the ribose 3′-OH was not clear with substrate assisted catalysis, a catalytic residue, and metal activation all possible. Substrate assisted catalysis is shown theoretically to be a factor in the transphosphorylation catalyzed by RNase A[6] and is widely observed in enzyme catalysis of phosphate hydrolysis.[7,8] The available aspartate base residues are involved in binding to the metals and it was not clear they can also bind and activate the 3′-OH. The function of each metal along the reaction path cannot be discerned from the structures because none has been obtained for transition state analogues. The details of product formation through a five-coordinate intermediate are speculative with concern that the isolated cAMP structure is not compatible with the active site geometry.[1] Leveraging the reaction path from the structure of the bound substrate analogue by theoretical calculation provides detailed structural information for the reacting complex as well as specific details regarding the electronic and structural interactions within the active site.

The crystal structure with adenosine 5′-(α-thio)-triphosphate (R_p) (ATPα-R_p) bound in the active site will serve as the basis for the analysis and subsequent theoretical calculations.[1] The presence of two metals in the binding of the substrate immediately suggests the comparison to the reactive mechanism in polymerases.[9] The substrate model is formed from the thio R_p inhibitor by changing sulfur to oxygen and subsequent quantum mechanical energy optimization of the ATP in the

* Corresponding author. E-mail: krauss@carb.nist.gov.
[†] National Institutes of Health.
[‡] NIST.

10.1021/jp036564h
Published on Web 03/13/2004

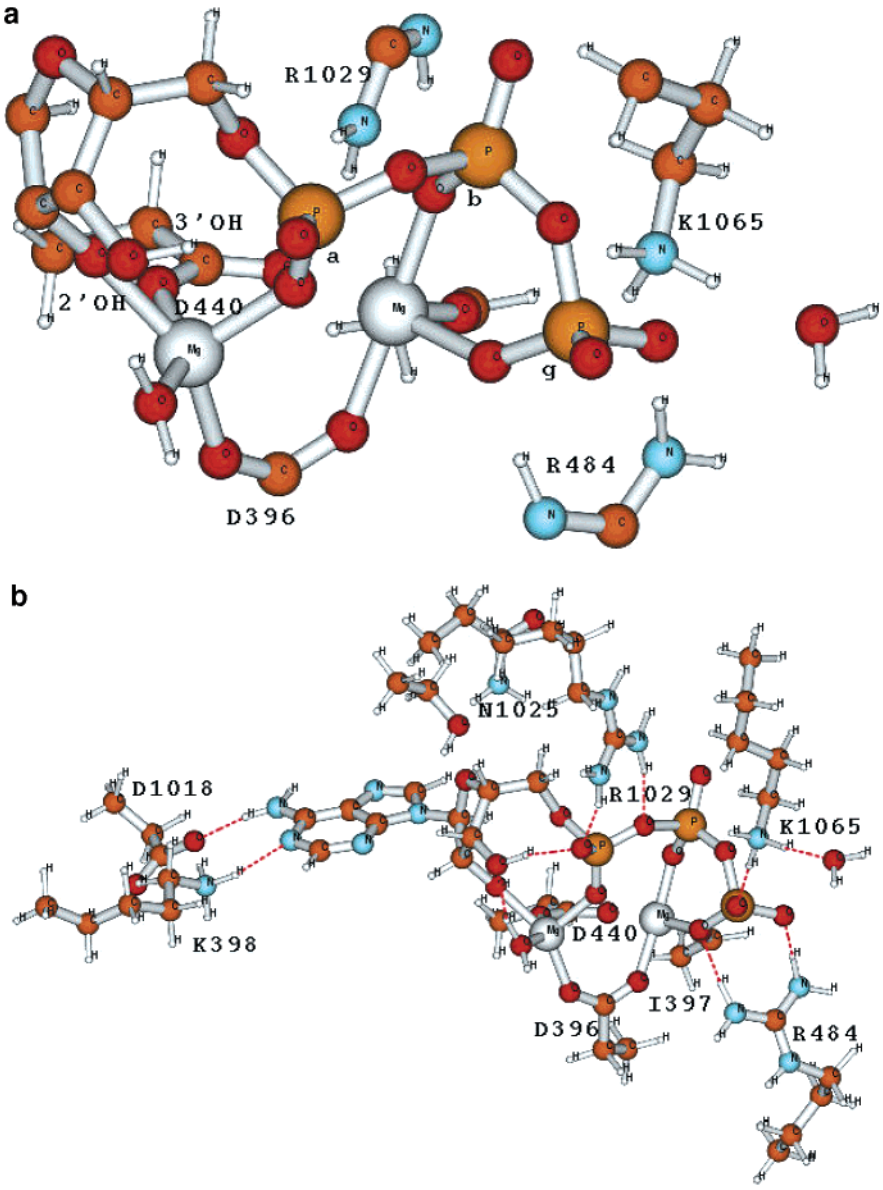

Figure 1. (a) Reactant complex showing the activation of 3′OH by the Pα phosphate oxygens, the catalytic MgA cation positioned by the bimetallic cluster with binding to D396 and D440. The phosphorus α, *β*, and *γ* atoms are designated a, b, and g. (b) Binding of ATP in adenyly cyclase active site showing lys, asp specificity to adenine; 3′OH H-bond to water and to Pα oxygen atoms; and two-Mg^{2+} cluster maintaining 3′O close to Pα and binding across the three phosphate groups.

active site. However, this structure does not yield 3′OH close to the site A metal. The substantial distance of the 3′OH from the metal is related to the orientation of the ribose hydroxyl groups in the refinement of the crystal structure. The X-ray refinement is not determined entirely by the electron density because the ribose is disordered in the structure. It is also possible that the orientation is true but describes the orientation of an inhibitor and not a reactive conformer. ATP may bind in a number of orientations but only one is reactive. The R_p oxygen of the thio S_p conformer is active, which also suggests that the ribose orientation must be altered. A possible reactive model was constructed from the X-ray structure[1] with the 3′OH within 2 Å of the metal in site A. However, we shall see that a quantum optimized structure does not find that 3′O can approach MgA that close. Nonetheless, a modified two-metal catalysis mechanism can be determined from theoretical calculations that involve a combination of phosphate activation of the 3′OH and metal cation stabilization of the developing charge on 3′O, as described in Figures 1a and 2a. Shifts in the relative binding of arginine residues to the triphosphate will also contribute to the stabilization of the reaction intermediate.

2. Method

The initial structure was obtained from the crystal structure of adenylyl cyclase with the R_p thiophosphate bound in the active site. The crystallographic ribose was rotated to position the 3′-OH group closer to the site A metal cation. The ribose hydroxyl groups are now positioned to interact with phosphate Sp oxygen atoms. The physiologically relevant Mg cations were substituted for the presumed crystallographic Zn and Mn cations. The sulfur atom is changed to oxygen and the entire model energy gradient optimized in the Hartree−Fock (RHF) approximation using the GAMESS suite of codes[10] with the Cα of the protein residues constrained. The initial positions of the ATP and the metals were chosen from the 1CJK structure[1] in the protein data bank.[11] Those residues bound to the ATPαS in the crystal structure were kept in the model. Two residues, asp1018 and lys938, determine the specificity to adenine. Three

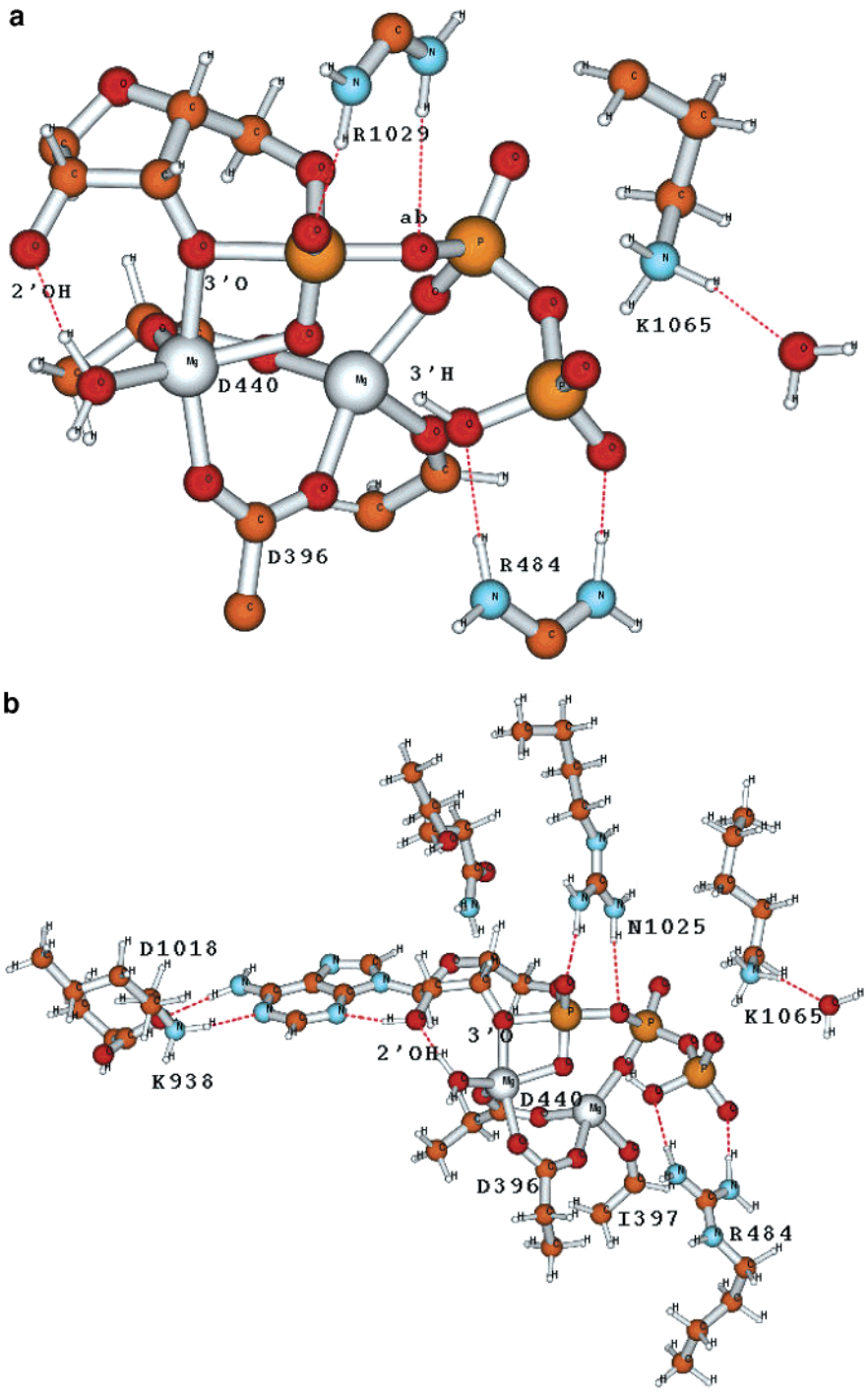

Figure 2. (a) Reactive intermediate complex with 3′O incorporated into cyclic phosphate and bound to MgA. The 3′H proton has moved to the Pγ oxygen and is within attacking distance of the Pα and Pβ bridging oxygen (Oab). (b) Reaction intermediate showing the formation of the cyclic phosphate incorporating 3′-O with reorganization of the metal cluster shifting coordination numbers between MgA and MgB.

residues, asp396, ile397, and asp440, are calculated as first shell ligands in the two-metal complex. Asn1025 is hydrogen bound to the ring oxygen in the ribose. Three cationic residues, arg484, arg1029, and lys1065, are bound to the triphosphate. The fundamental assumption of this calculation is that the side chains will move when the sulfur and metals are changed but that the backbone of the protein is essentially unchanged. The binding of other inhibitors can be used to validate this assumption. The dideoxyatp inhibitor is bound at the active site in the structure, 1CJT. Bond distances in the optimized reactant structure obtained starting from the 1CJK structure are compared in Tables 1 and 2 with the comparable bonds found in the 1CJK structure. The relevant comparison contains only the bonds made to the triphosphate.

Proton sharing between ion-pair moieties such as lys1065 with the Pγ oxygen can be resolved with water binding to an ammonium hydrogen. Only one water can bind because the ammonium makes two H-bonds to the phosphate. The calculated structures presented here along the reaction path all had one water bound to lys1065. The metal−ligand binding distances along the reaction path are shown in Table 3. An asp1018−lys938 ion pair also provides hydrogen binding and specificity to the adenine. Hydrogen binding of lys938 to the adenine maintains the ammonium cation on the lysine.

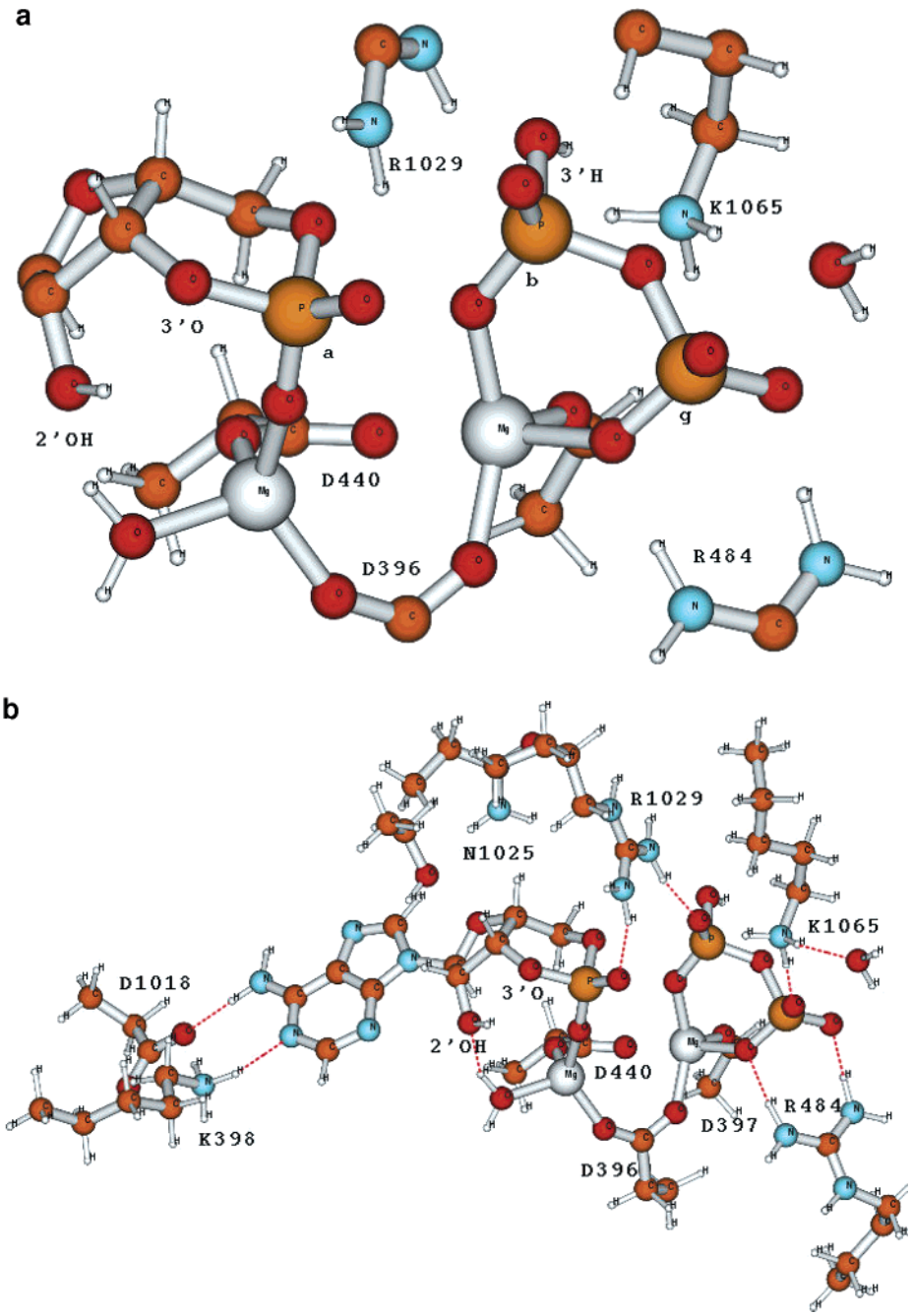

Figure 3. (a) The cAMP and pyrophosphate products are separated but still bound together by the bimetal complex and also weakly by H-bonds from arg1029. (b) cAMP and pyrophosphate products are constrained in the active site by H-bonds and bonds to the metal cluster with only the metal cluster showing strong bonds across the two products.

Effective core potentials were used to reduce the number of basis functions to 920 for the 193 atoms in the model.[12] The concomitant CEP-31G basis set was used to represent the atomic wave functions. The energy optimization was not driven to the default value of 0.0001 for the root-mean-square of the gradient because that would take considerable computer time for a system with many low-frequency modes. The iterative convergence was stopped when the energy change between steps dropped below 0.0002 hartrees. This energy difference is considerably smaller than the energy difference calculated along the reaction path. Because the default energy gradient was not used, the bond distances are only given to one place after the decimal.

After the reactant conformation was optimized (see Figure 1), the attack of the 3′OH was initiated by extending the 3′H proton toward the Sp oxygen for the α phosphate and lengthening the ribose C−O3 bond by 0.5 Å. If the 3′OH bond length is not sufficiently extended, the bond will re-form but when the OH bond is extended to about 2 Å, a five-coordinate intermediate ultimately is obtained with the formation of a cyclic phosphate, as seen in Figure 2. The proton now on the Sp oxygen is then extended toward the Rp oxygen on the γ phosphate but then reorients and binds to the bridging oxygen between the α and β phosphates, which breaks the α−β bond, leaving us with the cAMP and pyrophosphate product seen in Figure 3. Descriptions of only the atoms directly involved in the reactive complex are provided in Figures 1a, 2a, and 3a for clarity. In Figures 1b, 2b, and 3b the binding of the reacting complex to all the protein residues defining the catalytic site is

TABLE 1: Comparison of Bond Distances (Å) between Energy Optimized Native ATP Reactant and Dideoxyatp in the 1CJT Structure

Binding to MgA Site		
	CJT(Mg)	Opt(MgA)
Mn(MgB)	3.3	3.6
O(Pα)	2.0	2.0
OD1 asp440	2.0	2.0
OD2 asp440	3.3	3.3
OD1 asp396	2.4	2.0
OD2 asp396	3.2	3.3
O(Wat)	3.0	2.0
	CJT(Mn)	Opt(MgB)
O(Pα)	2.5	2.5
O(Pβ)	2.2	2.1
O(Pγ)	2.1	2.1
OD1 asp440	3.5	3.7
OD2 asp440	2.1	2.2
OD1 asp396	3.6	3.6
OD2 asp396	2.0	2.0
O ile397	2.2	2.1

TABLE 2: Comparison of Triphosphate Binding (Å) to arg1029, arg484, and lys1065 between 1CJT and Optimized Structures

		CJT	Opt
NH1 R1029	O1α	2.8	2.7
NH1 R1029	O3α	4.2	4.3
NH2 R1029	O2β	3.2	3.0
NH2 R484	O2γ	3.0	2.8
NH1 R484	O2γ	4.0	3.8
NH1 R484	O3γ	3.1	2.7
Nz K1065	O1γ	2.8	2.7

TABLE 3: Comparison of the Binding (Å) in the Metal Complex along the Reaction Path Structures

	reactant	intermediate	product
	MgA		
MgB	3.6	3.4	3.9
Oδ1- 440	2.0	2.0	2.0
Oδ2- 440	3.4	3.3	3.3
W1	2.0	2.0	2.0
Oδ1- 396	2.0	2.0	1.9
PαO	2.0	2.0	1.9
2′O	2.2	3.5	3.6
3′O	3.7	2.1	4.2
	MgB		
Oδ2- 440	2.2	2.0	2.2
Oδ2- 396	2.0	2.0	2.0
PαO	2.6	2.2	4.1
PβO	2.0	1.9	2.0
PγO	2.1	3.2	2.0
Oile	2.1	2.1	2.0
PγO- -N	2.6	2.5	2.6

depicted with all atoms included. The coordinates for the structures in Figures 1b, 2b, and 3b, are given in the Supporting Information.

3. Results

Reactant Binding. Binding distances of the optimized reactant conformation for comparable atoms in the substrate to the metal complex and the arginine residues 484 and 1029 agree well with those found for dideoxyatp analogue given in structure 1CJT, as seen in Tables 1 and 2. Reasonable agreement between these bond distances is found even with Mn and Mg as the metal pair in the 1CJT X-ray structure. The only bond distance that is substantially different is for the oxygen (water) distance to MgA, but the 1CJT structure has no hydroxyl groups on the sugar so the H-bond of the ligated water to 3′OH does not exist in 1CJT, distorting the binding of the water**.** The overall binding of the phosphate in the active site is also very similar in all analogue binding structures, 1CJK, 1CJT, 1CJU, and 1CJV. This demonstrates that the reaction path calculation can be initiated from any of these analogues and freezing the Cα backbone atoms.

For the reactive ribose conformation obtained in the theoretically optimized reactant in the active site, 3′OH is H-bonded to O(Pα)Sp with the H3 to O distance of 1.7 Å. This proton is necessarily close then to all three Pα phosphate oxygens with the other two oxygens 2.7 and 3.4 Å away. Neither MgA nor the carboxylate oxygens of asp440 are calculated bound to 3′OH. The OD1 oxygen of asp440 that is bound to MgA is H-bonded to 2′OH (1.7 Å), which is also bound to MgA. The water that is bound to MgA has a H-bond to O3′. This is all shown in Figure 1a. O3′ cannot get closer to MgA because of the bond between the α phosphate Rp oxygen to MgA and the orientation of the ribose ring. MgA has ionic bonds to the two asp ligands, 396 and 440, and one ionic bond to the phosphate. The ionic character of the Mg complex is evident from the calculated small bond orders for Mg bound to all the ligand oxygens. The bond orders are of the order of 0.1 for all the Mg−O bonds in the complex. The neutral 3′-OH cannot compete energetically with these ionic ligands and interacts with MgA only through the H-bond to the water bound to MgA.

MgA is a five-coordinate complex whereas MgB is a very distorted five- or six-coordinate complex. The OD2 oxygen of asp440 has a bond distance of 3.3 Å to MgA; this is not considered a sixth bond, but O(Pα) can be considered a sixth ligand to MgB with the distance 2.6 Å. The carboxylate oxygens from asp440 and asp396 that bind directly to MgB crowd the space around MgA and prevent additional water from binding to MgA. The bond distance of O(Pα)Rp to MgA is 2.0 Å and to MgB it is 2.6 Å. MgA and MgB are kept within 3.6 Å by the bridging carboxylate bonds of asp396 and asp440, which also limits ligand binding around the direction between the metals. The asymmetric bidentate bond of asp440 to both MgA and MgB can reorient and play a role in the stabilization of the reactive intermediate. There are strong H-bonds from arg1029 to O(Pα)Sp and the bridging oxygen between the α and β phosphate groups.

The most important and new determination from the optimization of the native reactant within the active site is that H3 is within short contact of all three O(Pα) atoms and O3 is 3.3 Å from Pα. H3 is attracted to all the oxygen atoms on the phosphate group. The reactant conformation maintains the close contacts for the 3′OH dissociation and attack on Pα, but the MgA does not polarize OH3 significantly. The more significant interaction is the attraction of H3 to the three O(Pα) atoms with one H to O distance of 1.7 Å.

Binding of the protein to adenine is primarily through strong ionic H-bonds of an aspartate to the amine of the pyrimidine ring and the lysine to the lone-pair electrons of N1. The lysine and aspartate are also bonded together in a salt-bridge. This is observed in the crystal structure and maintained in the course of the energy gradient optimization.

Intermediate Formation: 3′-OH Attacks Pα. The O(Pα)-Sp atom attracts and initially abstracts the H3 proton. An intermediate with H3 bound to O(Pα)Sp and the anionic 3′O H-bonded to the water bound to MgA does not form because the proton will not stay bound to the Sp oxygen due to the repulsion from the arginine H-bond. When the polarized 3′O is

directed toward the Pα, the reaction to form a cyclic phosphate occurs and results finally in the intermediate of Figure 2. The initial approach of the H3 proton first attaches in an energetically unfavorable manner to the Sp oxygen from Pα, but then moves toward the O(Pα)Rp bound to MgA. This proton then rotates during the energy gradient optimization to orient toward the Pγ oxygen. With the proper orientation the proton transfers, without a barrier, to bind to PγO, as depicted in Figure 2a. The H on PγO is within the same H-bond distance of 2.5 Å to both O$\alpha\beta$ and PαO.

A strong bond develops between the anionic 3′O and MgA that stabilizes the cyclization reaction. The phosphate is also rotated in such a way that the H-bond from arg1029 to the α phosphate oxygen is strengthened (1.7 Å) whereas the H-bond from arg1029 weakens (2.4 Å) to the β phosphate oxygen. This prepares the system for the next step that is the transfer of the 3′H proton to the bridging oxygen between Pα and Pβ that is no longer strongly bonded by the arg1029. Only MgA contributes strongly to the stabilization of the five-coordinate intermediate and transition state with a bond distance of 2.1 Å to 3′O. These changes in bonding distances aid in the formation of a stable five-coordinate intermediate that is 6 kcal/mol lower than the energy of the reactant.

Both asp396 and asp440 now bridge the MgA and MgB symmetrically and the formation of the additional ionic bond to the cyclic phosphate O3′ shortens the distance between the Mg cations by about 0.2 Å. The five-coordinate MgA complex for the reactant remains the same by replacing the loss of the bond to 2O′ with the formation of the MgA-3O′ bond. The MgB six-coordinate complex coordination reduces from six to five with the loss of the bond to O(Pγ). The formation of the cyclic phosphate is accompanied by closer binding interactions within the ligand cluster. The orientation of 2′OH of the ribose changes substantially with the MgA bond to 2O′ broken so that a H-bond is donated to N3 of the adenine and one accepted from the water bonded to MgA. If the water bound to lys1065 is removed, 3′H binds to O(Pα)Rp. The shift in the 3′H proton alters the metal binding to O(Pγ) and O(Pα)Rp substantially but does not affect the other heavy atom bond distances in the metal complex.

Product: cAMP + Pyrophosphate. The transfer of the H3 proton from PγO to the bridging oxygen between Pα and Pβ creates the products, cAMP and the pyrophosphate. The next most significant observation is the breaking of the bond between MgA and the 3′O within the cyclic phosphate with the distance in the intermediate of 2.1 Å increasing to 4.2 Å in the product. The Mg cations are still bridged by the asp396 and the MgA−MgB distance lengthens to 3.9 Å relative to the value of 3.6 Å calculated for the binding of the reactant. MgA and MgB both lose bonds found in the initial substrate conformation with MgA losing the bond to 2′O whereas MgB loses the bond to PαO. The other bonding interaction to the phosphates that changes is for arg1029 that is now H-bonded strongly to only the cAMP. The product structure is about 3 kcal/mol less stable than the substrate complex at this stage of the optimization. Shifting of the position of the shared proton between lys1065 and the phosphate by removing the water bound to the lysine has essentially no effect on the overall structure of the bound product.

4. Comparison with Experimental Mechanism

The binding site is constructed from residues donated from two cyctoplasmic domains that contribute to the structure of adenylyl cyclase.[13] However, once the active site is formed, most of it is relatively rigid because of all the ionic bonds between the residues, metals, and substrate. Most water of hydration of the polar and ionic constituents is squeezed out when the reactive active site is formed with hydrophobic groups packed around the base and sugar.[2] The ATP binding is at one end of a groove that is capped by the lysine bound to the γ phosphate.[2] The X-ray structures with different reactant analogue inhibitors, 1CJK and 1CJT, differ slightly in the protein residue structure binding the inhibitors. However, the similarity in the bond distances for the binding of the comparable phosphate moiety given in Tables 1 and 2 between the calculated native ATP and the dideoxyatp analogue in 1CJT shows that allowing flexibility only in the residue side-chains yield very similar phosphate binding.

The two-metal crystal structure immediately suggests that the reaction proceeds analogously to the polymerase reaction.[2,9] However, the atomic level mechanism for activation of 3′OH is not evident from the experimental structures and there is no prediction of the reaction intermediates or the structure of the final product complex. In the experimental structure the mammalian adenylyl cyclase has no obvious base that can abstract the 3′H proton. The calculated two-metal reactant conformation shows that the asp396 and asp440 are not able to move away from the metals to approach and activate 3′OH. If MgA is removed, then the situation changes but experimentally the presence of two metals is found necessary for activity.[14,15] Substrate assisted catalysis has also been suggested for this reaction.[5,16] This is, in fact, what is calculated for the first step in the reaction path. The presence of the arginine ionic H-bonding prevents 3′H proton transfer to the O(Pα)Sp atom and directs this proton first to O(Pα)Rp, which is consistent with the activity observed for diastereo ATPαS isomers,[17] and then to PγO. There is a short H-bond from PγO to both O(Pα)-Rp and O$\alpha\beta$ so the intermediate is positioned for the final proton attack that creates the cAMP product. The substrate assisted five-coordinate reaction path calculated for polymerase β recently[18] used a model with arginine residues bound only to the γ phosphate so the difficulties encountered here in proton transfer because of the arginine binding also to the α and β phosphate are specific to the adenylyl cyclase reaction. The stereochemical activity relation could be tested with mutational replacement of the arginine ionic H-bonding.

Both metals are required for organizing the substrate for the 3′OH attack with the primary catalytic metal in site A. Even the water bound to MgA helps to orient the 3′H proton toward the phosphate oxygens. The coordination geometry of the Mg cations is calculated to be 5 for strongly bound ligands in the reactant complex, but the OD2 atoms in the carboxylate groups of asp396 and asp440 are close enough to crowd the space around MgA. MgB also occupies space along a coordinate axis and prevents a larger coordinate number of strongly bound ligands. Mn binding for the dideoxyatp reactant analogues still finds the binding distances for the triphosphate binding is comparable to the calculated structure. This suggests that the differences observed in the stereochemical activity between Mg and Mn activated guanylyl cyclase[17] may not carry over directly to the properties of the adenylyl cyclase.

The reaction proceeds with inversion of configuration, in agreement with the in-line attack and formation of a five-coordinate intermediate.[17,19] The calculated reaction path is in agreement with this observation and provides structural five-coordinate intermediates bound to MgA and MgB that is a minimum on the reaction path. The product structure maintains the doubly bridged metal cation cluster with a relatively slight increase in the separation of the metals. The nearly perpendicular

orientation of adenine to the ribose in the bound reactant changes to a nearly parallel orientation in both the intermediate and the product. The Pα to bridging Oβ distance increases from 1.6 to 4.1 Å with a relatively small change in the metal cluster bond distances but a reorientation of the β and γ phosphates allowed by rearranging the arginine H-bonds. Solvating these bonds would allow water to access the metal cluster and initiate release of the products.

5. Conclusion

We have shown that a reactive native structure of ATP bound in the active site of adenylyl cyclase can be constructed from an inhibitor X-ray structure. This structure is energy optimized to provide the initial reactant structure along the reaction path. The lowest energy intermediate and the product structure along the reaction path are then obtained by further energy optimization. The calculations provide an atomic level description of the binding of the reacting complex in the native active site and the reaction mechanism. The activation of 3′OH is shown as autocatalytic with the 3′H proton abstracted by the Pα phosphate oxygens and the developing charge on 3′O stabilized by a strong bond with MgA in the reaction intermediate. The flexible coordination binding at MgA or in the two-metal complex helps drive the reaction from the intermediate to the product. The separated products, cAMP and pyrophosphate, are still bound by all the H-bonds that sequestered the reactant. The binding of cAMP in the product active site leads to the adenine rotated around the glycosidic bond about 90° relative to the optimized structure for the isolated cAMP.

Reactive binding requires that 2′OH and 3′-OH are reoriented from the X-ray conformation while retaining the stereo-arrangement for ATP. In the X-ray structure, 1CJK, the ribose was oriented as an inhibitor. Asn1025 remains bound to 4′O for the reactive ribose conformation and along the reaction path. The H-bond from 2′-OH is directed toward the OD1 of asp440 initially and toward 3′O in the product. But in the intermediate structure 2′OH is H-bonded to N3 of the adenine and does not seem to play any significant role in stabilizing the developing charge on 3′O as the proton is abstracted. The rearrangement of 3′OH from the X-ray inhibitor structure directs them toward the Pα phosphate oxygens with a short H-bond in the energy optimized reactant structure. The H-bonds to these phosphate oxygen atoms activates the 3′-OH bond with an autocatalysis step initiating the reaction.

The two-metal cluster rearranges the metal coordination along the reaction path. The coordination numbers of strong ligand binding for MgA and MgB are, respectively, 5,5 in the substrate conformation, 5,5 in the five-coordinate intermediate, and 4,5 in the product. The binding ligands to MgA in the intermediate change identity. This reflects the ability of the two-metal cluster to respond to the changing charge rearrangement along the reaction path. The coordination numbers do not consider weak bidentate binding from the aspartate carboxylates or the close interaction between the two metal cations. The coordination flexibility in site A permits this Mg to play a catalytic role in stabilizing the developing transition state and reactive intermediate. Although MgA does not play a role in activating the 3′OH bond in the reactant, the MgA-3′O bond forms in the reactive intermediate.

A catalytic role is found for both MgA and the Pα oxygen atoms. Abstraction of the proton from 3′-OH is initiated by the phosphate oxygens, but the attraction of 3′O to MgA would seem to be the ultimate driving force. The two-metal cluster organization is also required to maintain the appropriate MgA position and so is necessary for efficient catalysis. There is no role found for either of the aspartate bases bound in the metal cluster specifically for catalysis. Proton transfers between the various phosphate groups required for breaking the bond to cAMP occur with low or no barriers in the course of just energy optimizations. Flexible arginine hydrogen binding across the phosphate bonds along the reaction path also differentially stabilizes the energy of the intermediate and product. The arginines can be considered as catalytic residues in this sense.

The final product is still constrained in the active site by a number of H-bonds with both the two-metal cluster and arg1029 binding across the cAMP and pyrophosphate groups of the product. The product complex is 3 kcal/mol higher in energy than the reactant whereas the five-coordinate intermediate is 6 kcal/mol more stable than the reactant. Activation energy and transition state calculations can now be based on this reaction path with the inclusion of the protein environment. Distortion of the cAMP and phosphate orientations may open the site sufficiently to water to weaken the binding to the two-metal cluster and thus release product. The questions posed in the Introduction regarding the detailed mechanism can be answered by ab initio quantum chemical calculation by leveraging an X-ray analogue binding structure into a native substrate bound in the active site. The calculated structures along the reaction path can be used for templates to model inhibitors specific to reaction path binding.

The specificity of the binding to the adenine base shown in the X-ray structure of the analogue is maintained through the native reaction path. The lysine and aspartate residues must both be present to prevent the possibility of the lysine transferring a proton to the adenine. Orientation and binding distances of the triphosphate to the residues in the active site does not seem to depend on small differences in the active site of different reactant analogue inhibitors.

Acknowledgment. M.K. is grateful to Dr. Bernard R. Brooks for providing access to the Biowulf PC/Linux cluster at the National Institutes of Health, Bethesda, Md. This study utilized the high-performance computational capabilities of the Biowulf PC/Linux cluster at the National Institutes of Health, Bethesda, Md. (http://biowulf.nih.gov).

Supporting Information Available: Cartesian structure coordinates. This material is available free of charge via the Internet at http://pubs.acs.org.

References and Notes

(1) Tesmer, J. J.; Sunahara, R. K.; Johnson, R. A.; Gosselin, G.; Gilles, G.; Gilman, A. G.; Sprang, S. R. Two-metal-Ion catalysis in adenylyl cyclase. *Nature* **1999**, *285*, 756−760.

(2) Hurley, J. H. Structure, mechanism, and regulation of mammalian adenylyl cyclase. *J. Biol. Chem.* **1999**, *274*, 7599−7602.

(3) Tesmer, J. J.; Dessauer, C. W.; Sunahara, R. K.; Murray, L. D.; Johnson, R. A.; Gilman, A. G.; Sprang, S. R. Molecular basis for P-site inhibition of adenylyl cyclase. *Biochemistry* **2000**, *39*, 14464−14471.

(4) Tang, W. J.; Stanzel, M.; Gilman, A. G. Truncation and alanine-scanning mutants of type I adenylyl cyclase. *Biochemistry* **1995**, *34*, 14563−14572.

(5) Yan, S. Z.; Huang, Z. H.; Shaw, R. S.; Tang, W. J. The conserved asparagine and arginine are essential for catalysis of mammalian adenylyl cyclase. *J. Biol. Chem.* **1997**, *272*, 12342−12349.

(6) Wladkowski, B. D.; Krauss, M.; Stevens, W. J. Transphosphorylation catalyzed by ribonuclease A: Computational study using ab initio effective fragment potentials. *J. Am. Chem. Soc.* **1995**, *117*, 10537−10545.

(7) Schweins, T.; Geyer, M.; Scheffzek, K.; Warshel, A.; Kalbitzer, H. R.; Wittinghofer, A. Substrate-assisted catalysis as a mechanism for GTP hydrolysis of p21ras and other GTP-binding proteins. *Nat. Struct. Biol.* **1995**, *2*, 36−44.

(8) Kosloff, M.; Selinger, Z. Substrate assisted catalysis - - application to G proteins. *Trends Biochem.; Sci.* **2001**, *26*, 161−166.

(9) Steitz, T. A. DNA polymerases: structural diversity and common mechanisms. *J. Biol. Chem.* **1999**, *274*, 17395−17398.

(10) Schmidt, M. W.; Baldridge, K. K.; Boatz, J. A.; Elbert, S. T.; Gordon, M. S.; Jensen, J. H.; Koseki, S.; Matsunaga, N.; Nguyen, K. A.; Su, S. J.; Windus, T. L.; Dupuis, M.; Montgomery, J. A. General Atomic and Molecular Electronic-Structure System. *J. Comput. Chem.* **1993**, *14*, 1347−1363.

(11) Berman, H. M.; Westbrook, J.; Feng, Z.; Gilliland, G.; Bhat, T. N.; Weissig, H.; Shindyalov, I. N.; Bourne, P. E. *Protein Data Bank Nucl. Acids Res.* **2000**, *28*, 235−242.

(12) Stevens, W. J.; Basch, H.; Krauss, M. Compact Effective Potentials and Efficient Shared Exponent Basis Sets for the First- and Second-Row Atoms *J. Chem. Phys.* **1984**, *81*, 6026−6033.

(13) Krupinski, J.; Coussen, F.; Bakalyar, H. A.; Tang, W. J.; Feinstein, P. G.; Orth, K.; Slaughter, C.; Reed, R. R.; Gilman, A. G. Adenylyl cyclase amino acid sequence: possible channel- or transporter-like structure. *Science* **1989**, *244*, 1558−1564.

(14) Pieroni, J. P.; Harry, A.; Chen, J.; Jacobowitz, O.; Magnusson, R. P.; Iyengar, R. Distinct characteristics of the basal activities of adenylyl cyclases 2 and 6. *J. Biol. Chem.* **1995**, *270*, 21368−21373.

(15) Zimmermann, G.; Zhou, D.; Taussig, R. Mutations uncover a role for two magnesium ions in the catalytic mechanism of adenylyl cyclase. *J. Biol. Chem.* **1998**, *273*, 19650−19655.

(16) Tesmer, J. J.; Sunahara, R. K.; Gilman, A. G.; Sprang, S. R. Crystal structure of the catalytic domains of adenylyl cyclase in a complex with Gsalpha. GTPgammaS. *Science* **1997**, *278*, 1907−1916.

(17) Koch, K. W.; Eckstein, F.; Stryer, L. Stereochemical course of the reaction catalyzed by guanylate cyclase from bovine retinal rod outer segments. *J. Biol. Chem.* **1990**, *265*, 9659−9663.

(18) Abashkin, Y. G.; Erickson, J. W.; Burt, S. K. Quantum chemical investigation of enzymatic activity in DNA polymerase β. A mechanistic study. *J. Phys. Chem. B* **2001**, *105*, 287−292.

(19) Gerlt, J. A.; Coderre, J. A.; Wolin, M. S. Mechanism of the adenylate cyclase reaction. Stereochemistry of the reaction catalyzed by the enzyme from Brevibacterium liquefaciens. *J. Biol. Chem.* **1980**, *255*, 331−334.